

Structural and spectroscopic characterization of Ho³⁺ in sol-gel silica

P. R. REJIKUMAR, PRATHIBHA VASUDEVAN, S. KARTHIKA, J. GEORGE^a, N. V. UNNIKRISHNAN*

School of Pure & Applied Physics, Mahatma Gandhi University, Kottayam-686 560, INDIA

^aDepartment of Physics, Christian college Chengannur, Kerala- 689122, INDIA

Ho³⁺ doped silica glasses were prepared by the sol-gel process using tetraethyl orthosilicate (TEOS), H₂O, HNO₃ and Ho(NO₃)₃·6H₂O. The samples were characterized using thermo gravimetric analysis (TGA), FTIR spectra, high resolution transmission electron micrograph (HRTEM) and UV-VIS absorption spectra. Judd-Ofelt (JO) ($\Omega_2= 4.480 \times 10^{-20} \text{ cm}^2$, $\Omega_4=2.292 \times 10^{-20} \text{ cm}^2$, $\Omega_6=2.827 \times 10^{-20} \text{ cm}^2$) parameters were derived from the optical absorption spectra. Calculated values of the J-O parameters were utilized in evaluating the various radiative parameters such as electric dipole line strengths (S_{ed}), radiative transition probabilities (A_{RAD}), radiative lifetimes (τ_{RAD}), fluorescence branching ratios (β_R) and the integrated absorption cross sections (σ_a) for stimulated emission of Ho³⁺ ion. Our analysis indicates that randomly distributed three dimensional network nature of the host, clustering of Ho³⁺ ions and the hydroxyl content are responsible for the weak fluorescence. Also asymmetry of Ho³⁺ in silica glass host is found to be higher than those in halide systems and lower than oxide systems

(Received March 31, 2010; accepted May 26, 2010)

Keywords: Glasses, sol-gel growth, Electron microscopy, FTIR spectroscopy

1. Introduction

Optical properties of rare earth ion doped glasses are widely investigated for potential applications in optical devices [1]. Rare earth ions have a number of efficient and narrow emission lines in the visible and NIR wavelength regions whose position is insensitive to their matrices due to the shielding effect of 5s and 5p electrons. Rare earth doped glasses, play an important role for optical applications such as glass lasers and optical fiber amplifiers and also hold promise for photochemical hole-burning memory, flat panel displays etc [2]. The potential advantages of the sol-gel method for preparing optical materials include obtaining new chemical compositions, better purity and more convenient processing conditions [3]. The optical absorption and luminescence properties of several rare earth ions incorporated into sol-gel silica have been reported [4,5]. Ho³⁺ doped glasses were first reported, 30 years ago, by Reisfeld et al [6] with emphasis on visible and near-infrared emission. Since then, the qualities of the glasses have improved considerably. Development of such functional glasses requires detailed microscopic information, especially on the local structures around the rare earth ions. A study of the incorporation of Ho³⁺ ions in sol-gel silica host is yet to be well established. The aim of the present study is (i) to characterize Ho³⁺ doped silica glass by TGA, FTIR, HRTEM and absorption spectroscopy (ii) to confirm the clustering of rare-earth ions in pure silica matrix (iii) to obtain various radiative properties of Ho³⁺ in sol-gel silica from Judd-Ofelt calculations (iv) to show the fluorescence quenching mechanism in three dimensional random silica network.

2. Experimental

Silica sols containing 1.0 equivalent mol% Ho₂O₃ were prepared from tetraethylorthosilicate (TEOS) (Fluka purum grade), Ho(NO₃)₃·6H₂O (Sigma Aldrich), doubly distilled deionised water and highly pure HNO₃ and NH₄OH. The desired amount of Ho(NO₃)₃·6H₂O dissolved in deionised water in the presence of HNO₃ was poured into TEOS under stirring at room temperature. The TEOS/H₂O/HNO₃ molar ratio was 1:12:0.01. The pH of the sols was adjusted to a value of 3 by adding NH₄OH. The sols were cast in petridishes. The gels were aged for six weeks at room temperature. The gels were then heated at different temperatures ranging from 200-1000°C in a programmable furnace with a heating rate of 3°C per hour. Transparent, crack and bubble free gels (diameter 20-25 mm, thickness 2-2.5 mm) were reproducibly obtained. Optical absorption and emission spectra of the heat treated sample were recorded with UV-visible spectrophotometer (Shimadzu-UVPC2401) and spectro-fluorophotometer (Shimadzu- RFPC 5301). The lifetime measurements were done using a Tektronix storage oscilloscope (THS730A). Thermo gravimetric curve was recorded by a Shimadzu Thermal Analyser DT 40 under N₂ atmosphere. X-ray diffraction pattern was recorded on a Shimadzu X-ray diffractometer with CuK α radiation. The HRTEM micrographs are obtained using a JEOL 3010 instrument with a lattice resolution of 0.14 nm and a point-to-point resolution of 0.12 nm. The FTIR spectrum of the sample in the region 400-4000 cm⁻¹ was recorded by using Shimadzu FTIR spectrometer 8400 S. Density of the sample was measured using Archimede's

principle. All measurements were done at room temperature.

3. Results and discussion

Fig.1 shows the thermo gravimetric (TG) curve of the 1 mol% Ho_2O_3 doped silica gel heated upto 1000°C . On heating the gel loses trapped volatiles below 200°C and a subsequent monotonic loss with increasing heat-treatment temperature is due to the removal of hydrogen bonded molecular water and dehydration via condensation of silanol group. At intermediate temperatures, the host structure exhibits inhomogeneity due to insufficient formation of siloxane bonds. Further formation of Si-O-Si network (1000°C) leads to the destruction of water sites of holmium and progression towards glassy structure [7]. Density of the gel heat treated at 1000°C was measured by Archimedes' method using alcohol as buoyant fluid. The 1.0 mol % xerogels had densities 2.21 g/cm^3 which agrees reasonably well with the theoretical densities of the corresponding glasses obtained from the mixing rule.

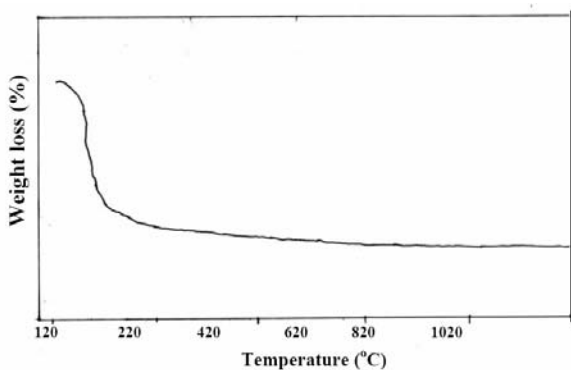


Fig. 1. TG curve of the 0.1mol% specimen.

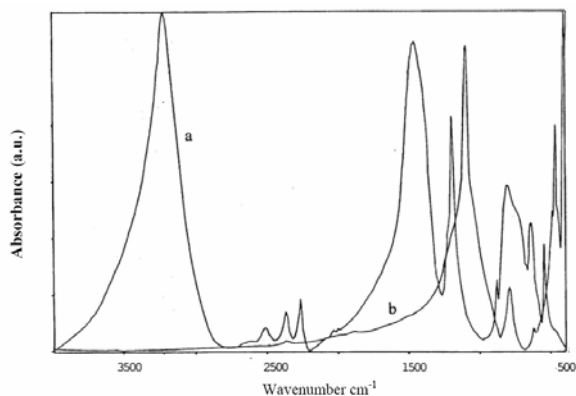


Fig. 2. FTIR spectra of the 500°C (a) and 1000°C (b) heated.

FTIR spectra of the silica gels at 60°C and 1000°C are shown in Fig 2. With the increase in temperature of heat treatment, the bands due to the presence of absorbed water

(3500cm^{-1} and 1600cm^{-1}) and residual organics (1450cm^{-1} and 1375 cm^{-1}) decrease in intensity. The 550cm^{-1} and 750cm^{-1} bands due to the structural defects and the 955 cm^{-1} owing to the Si-OH anti-symmetric stretching vibration have progressively weakened. During sol-gel processing one can always have fluctuations in the packing of the sample. These fluctuations often get amplified during the heat treatment process. This yields an inhomogeneous densification of the sample. Further, the differential stresses arising from inhomogeneous densification result in structural defects [8]. The characteristic bands associated with the various vibrational modes and structural defects are given in Table.1. The FTIR spectrum of the sample heat-treated at 1000°C is similar to that of the silica glass prepared by conventional methods [9]. FTIR spectrum of the 1000°C heat-treated specimen shows that a high temperature heat treatment can greatly reduce the amount of OH groups and organic residue in the silica glass. The amount of hydroxyl groups and the three dimensional silica network in the dense glass is primarily responsible for the weak fluorescence. As expected the sample does not show an appreciable fluorescence. The -OH impurity can be removed completely by a special dehydroxylation step during heat treatment of the gel [10].

Table 1. FTIR absorption bands and characteristic groups

Absorption frequency (cm^{-1})	Assignment
520	Si-O-Si bending mode
631	Structural defects
780	Si- O-Si symmetric stretching
1100	Si- O-Si symmetric stretching in cyclic structure
1420	Ethyl group, vibration modes
3200 (broad band)	OH vibrations of residual adsorbed water, Si-OH stretching and asymmetric C-H stretching

The HRTEM micrograph of the xerogel heat treated at 1000°C , shown in Fig.3, confirms the formation of clusters. Dopant clustering refers to the tendency of luminescent species to aggregate with it through oxygen linkages and is deleterious because it leads to concentration quenching of luminescence through cross relaxation and energy transfer processes [4]. The tendency to cluster can also lead to phase separation at high dopant concentrations normally desired for luminescence and lasing applications. The results of this study support the modified random network model of glass structure proposed by Greaves [11]. This model proposes that modifying cations are not distributed randomly in glass but rather that they have a tendency to aggregate locally with

some degree of ordering. The overall structure of the glass is proposed to consist of randomly distributed modifier rich regions and modifier deficient domains. The modifier rich domains are largely ionic while the modifier deficient regions are largely covalent and comprise predominantly network forming species. Both the halo of the electron diffraction pattern (Fig. 4) and the broad peak in the X-ray diffraction pattern (Fig. 5) confirm the amorphous nature of the matrix.

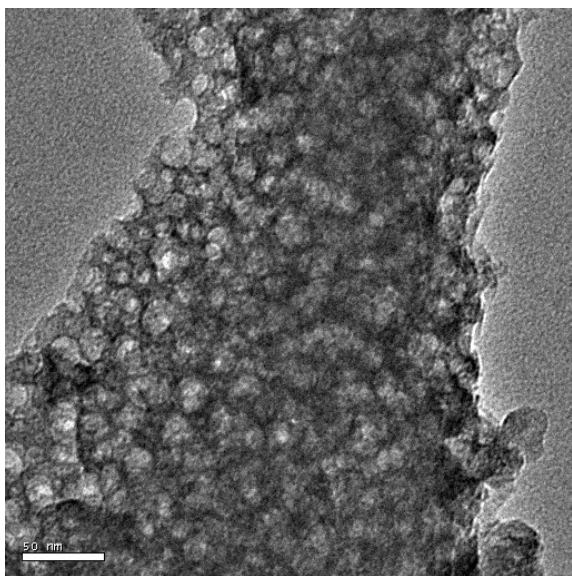


Fig. 3 HRTEM of holmium in sol-gel silica.

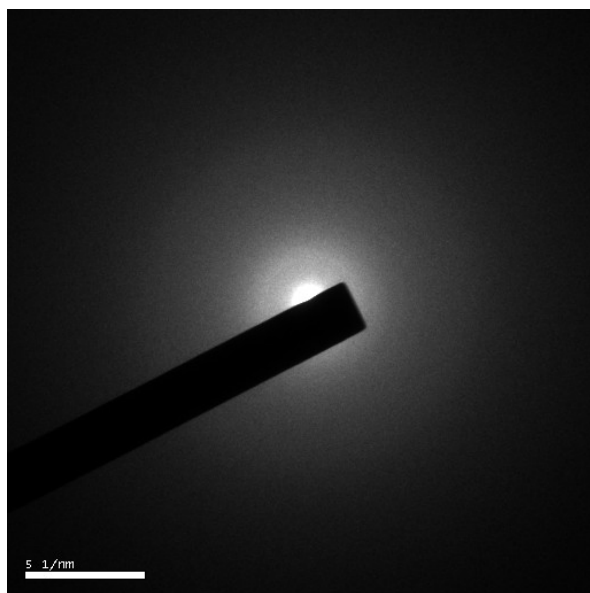


Fig. 4. Electron diffraction pattern Ho^{3+} doped silica.

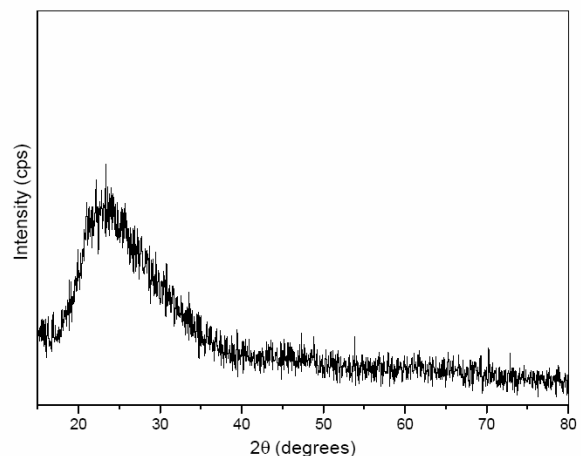


Fig. 5. X-ray diffraction pattern of Ho^{3+} in sol-gel silica.

UV-VIS absorption spectra of 1 mol% Ho^{3+} -doped xerogel fired at 1000°C is shown in Fig. 6. For the Ho^{3+} ion, the transition occurs from the $^5\text{I}_8$ level to various excited levels [12]. The electronic transitions of the trivalent lanthanides can be electric dipole, magnetic dipole or electric quadrupole in nature. Neglecting higher multipole mechanisms such as electric quadrupole transitions, oscillator strength (f) can be regarded as a sum of the electric dipole (f_{ed}) and magnetic dipole (f_{md}) contributions. Line strength of magnetic dipole (md) transitions is much less than the line strength of electric dipole transitions ($S_{JJ'}^{md} \ll S_{JJ'}^{ed}$). Therefore in radiative intensity calculations the electric dipole approximation is commonly used and magnetic dipole transitions are only taken into account if required [13].

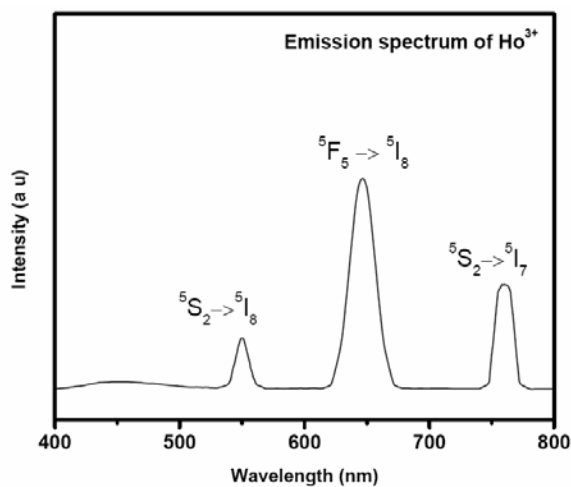


Fig. 7. Emission spectrum of Ho^{3+} doped silica glass

Oscillator strength (f) can be expressed in terms of the molar extinction coefficient (ϵ), and the energy of the transition in wave number (ν) by the relation [13].

$$f_{\text{exp}} = 4.32 \times 10^{-9} \int \epsilon(\nu) d\nu \quad (1)$$

The Judd-Ofelt [14,15] theoretical analysis is widely used in rare earth ion spectroscopy to model electric dipole f - f intensities. It allows to calculate any transition intensity between f multiplets once three parameters known as JO parameters are determined. According to JO theory

$$f_{\text{ed}} = \frac{\nu}{(2J+1)} \left[\frac{8\pi^2 mc (n^2 + 2)^2}{3h \cdot 9n} \right] \sum_{\lambda=2,4,6} \Omega_{\lambda} \langle \psi J \| U^{\lambda} \| \psi' J' \rangle^2 \quad (2)$$

where $(2J+1)$ is the degeneracy of the ground state, ν is the mean energy of the $|\psi J\rangle \rightarrow |\psi' J'\rangle$ transition, U^{λ} is a unit tensor operator of rank λ . The measured and calculated oscillator strengths and electric dipole line strengths of the experimentally observed transitions along with JO parameters are given in Table 2. Experimentally measured oscillator strengths and electric dipole line

strengths of various absorption transitions of Ho^{3+} ion and the JO parameters in the present glassy systems are found to be in good agreement with that of other oxide systems[9]. The JO parameters are important for investigations of local structure and bonding in the vicinity of rare earth ions. Ω_2 is related to asymmetry of glass hosts. In this case Ω_2 is larger than those in LaF_3 , YAlO_3 , ZnF_2 - CdF_2 systems but smaller than those in oxide systems like phosphate, borate, silicates, etc. These differences indicate that the asymmetry of Ho^{3+} silica glass host is higher than those in halide systems and lower than other oxide systems [12]. An immediate measure of the quality of the fit is given by the root mean square (r.m.s.) deviation between the measured and calculated oscillator strengths and electric dipole line strengths. It is defined as [16]

$$r.m.s. = \sqrt{\frac{\sum (f_i^{\text{exp}} - f_i^{\text{meas}})^2}{M - 3}} \quad (3)$$

where M is the set of experimental values. Small values of r.m.s. deviations in the present case clearly supports the accuracy of the JO theory.

Table 2. Measured and calculated oscillator strengths (10^{-6}), electric dipole line strength (10^{-20} cm^2), Judd-Ofelt parameters and bonding parameter of Ho^{3+} in the glass studied.

Transition from $^5\text{I}_8$	$f_{\text{mea}} (10^{-6})$	$f_{\text{cal}} (10^{-6})$	$S_{\text{mea}} (10^{-20} \text{ cm}^2)$	$S_{\text{cal}} (10^{-20} \text{ cm}^2)$
$^5\text{F}_5$	4.147	3.333	3.215	2.582
$^5\text{F}_4$	3.628	3.931	2.353	2.547
$^5\text{F}_3$	0.5616	1.675	0.328	0.978
$^5\text{G}_6$	16.84	16.750	9.157	9.138
$(^5\text{G}, ^3\text{G})_5$	1.598	2.427	0.8069	1.224
$^3\text{H}_6$	2.548	2.855	1.111	1.243
R.M.S	$\pm 0.939 \times 10^{-6}$		$\pm 0.610 \times 10^{-20}$	
Judd- Ofelt parameters	$\Omega_2 = 4.480 \times 10^{-20} \text{ cm}^2$, $\Omega_4 = 2.292 \times 10^{-20} \text{ cm}^2$, $\Omega_6 = 2.827 \times 10^{-20} \text{ cm}^2$			
Bonding parameter (δ)	- 0.1982			

Radiative transition parameters such as total radiative transition probability (A_T), radiative lifetime (τ_{RAD}), and the fluorescence branching ratio (β_R) are calculated using the known expressions [13].

For rare-earth ions, taking account of multiple terms splitting, its spontaneous radiative transition probability becomes

$$A_{JJ}^{ed} = \frac{64\pi^2 e^2 \nu^3}{3h(2J+1)} \left[\frac{n(n^2+2)^2}{9} \right] S_{ed} \quad (4)$$

As the coefficients for spontaneous emission equal the reciprocal radiative relaxation time,

$$A_{JJ}^{ed} = \tau_{Rad}^{-1} \quad (5)$$

$$\tau_{rad} = \frac{1}{\sum_{J'} A_{JJ'}} \quad (6)$$

The position of the lines in absorption or emission spectra seems to be independent of the surroundings. Their intensity ratios vary strongly, indicating certain selection rules, which are reflected by the branching ratio. The relative amplitudes of the fluorescence transitions or fluorescence branching ratio is given by

$$\beta_{JJ'} = \frac{A_{JJ'}}{\sum_{J'} A_{JJ'}} \quad (7)$$

The integrated absorption cross-section or effective cross-section (σ_a) for stimulated emission is estimated using the Fuchtbauer-Ladenberg equation [13]

$$\sigma_a = \frac{A(\psi J)}{8\pi c n^2 \nu^2} \quad (8)$$

This equation is relevant because it is used for calculating emission cross sections of laser active materials. It also helps us to determine the upper energy level life time for transitions to any lower-lying energy levels. Branching ratio is the ratio of the radiative transition probability to the total radiative relaxation rate. It measures the percentage of emission for a given transition from a state with respect to all other transitions from this state. The radiative transition probability, radiative life times, branching ratios and integrated absorption cross-section for stimulated emission of the sample are given in Table 3. The table clearly shows fourteen transitions. Out of these transitions only two transitions are found to be suitable for optical amplification and may be considered as promising ones for laser action. Therefore, these two transitions are selected on the basis of the following criteria. In order to select transitions suitable for optical amplification and laser action, transitions having radiative relaxation rates with more than 300 cm⁻¹, branching ratios greater than 50% and an energy difference of about 3000 cm⁻¹ between the emitting level and the next lower level are chosen. The excited atom will emit light when the difference between the two states exceeds the limited phonon energy which is very much essential in order to overcome non-radiative relaxation rates. In Table.3 transitions ⁵F₅→⁵I₈ and ⁵S₂→⁵I₈ have greater than 50% predicted branching ratios with energy difference greater than 3000 cm⁻¹. This indicates that Ho³⁺ ion possesses two laser transitions in the present system that is easy to excite.

Table 3. Radiative rates, radiative lifetimes, branching ratios and integrated absorption cross-section for stimulated emission of Ho³⁺ ion in sol-gel silica.

Transition from		Energy ν cm ⁻¹	$A_{J'}$ s ⁻¹	A_T s ⁻¹	τ_{rad} μ s	β (%)	σ_A (10 ⁻²⁰ cm ²)
⁵ I ₇	⁵ I ₈	5150	85.89	85.891	11642	100	201.59
⁵ I ₆	⁵ I ₇	3500	20.29	85.890	4557	9.249	103.13
	⁵ I ₈	8540	199.11			90.75	169.96
⁵ F ₅	⁵ I ₄	2300	0.05	2268.18	440	0.002	0.65
	⁵ I ₅	4350	8.35			0.36	27.47
	⁵ I ₆	6910	104.02			4.58	135.62
	⁵ I ₇	10410	422.62			18.63	242.77
	⁵ I ₈	15450	1733.13			76.41	451.98
⁵ S ₂	⁵ F ₅	2740	0.29	2856.65	350	0.010	2.41
	⁵ I ₄	5030	43.54			1.52	107.13
	⁵ I ₅	7090	44.18			1.54	54.72
	⁵ I ₆	9650	173.52			6.07	116.00
	⁵ I ₇	13150	1052.14			36.83	378.77
	⁵ I ₈	18190	1542.95			54.01	290.29

Photoluminescence measurements were carried out for the gel, heat treated at room temperature, 200°C and 500°C do not show any fluorescence. However, weak fluorescence is observed for the sample heat treated at 1000°C. The emission spectrum of Ho³⁺ under the excitation of 460nm is presented in Fig.7. Fluorescence was observed from ⁵S₂ → ⁵I₈ (550nm), ⁵F₅ → ⁵I₈ (647nm) and ⁵S₂ → ⁵I₇ (761nm) transitions. Lifetimes of these emission levels measured at 300K yielded values of 93μs, 142 μs and 68μs respectively. The observed weak fluorescence intensity is attributed to the presence of residual -OH group, clustering of Ho³⁺ ions and three dimensional network structure.

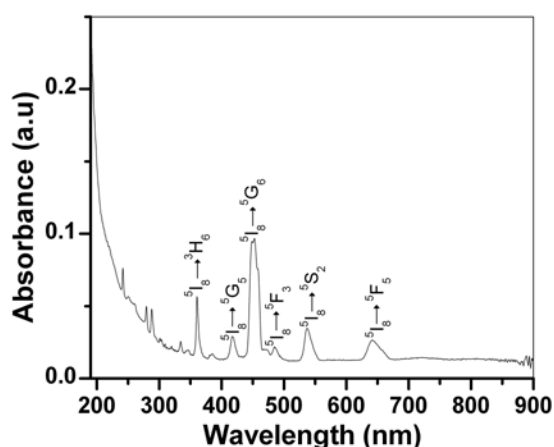


Fig. 6. Absorption spectra of 1mol%Ho³⁺ doped silica glass heat treated at 1000°C.

The bonding parameter (δ) defined as $\delta = \left[\frac{(1-\bar{\beta})}{\bar{\beta}} \right] \times 100$ where $\bar{\beta} = \sum \beta / N$ and $\beta = v_c / v_a$ (the nephelauxetic ratio), v_c and v_a are the energies of the corresponding transitions in the complex and aqua ion respectively, and N refers to the number of levels used to compute $\bar{\beta}$ values. Depending upon the environmental field, δ may be positive or negative indicating covalent or ionic bonding respectively. In the present study negative value of δ (-0.1982) clearly implies that the matrix is dominant with ionic bonding. This is in good agreement with the results obtained by earlier workers [4,13].

4. Conclusions

Sol-gel silica glass doped with Ho³⁺ ions was prepared. TGA analysis showed almost complete removal of molecular water and the condensation of silanol groups with heat treatment. FTIR analysis revealed all the vibrational modes present in the silica glass system. However, the vibrational modes corresponding to the structural defects and Si-OH bond were found to weaken

with heat treatment. The cluster formation is quite evident from the HRTEM micrograph. The JO parameters and the radiative parameters were evaluated and compared with similar matrices. The transitions ⁵F₅ → ⁵I₈ and ⁵S₂ → ⁵I₈ are found to have the potential for optical amplification. The negative value of the bonding parameter shows that ionic bonding is dominant in the matrix. The results presented here are in good agreement with the findings of earlier workers about the structure of glass and clustering of rare earth ions in sol-gel matrix.

Acknowledgements

Authors are thankful to University Grants commission (UGC), Government of India for assistance through SAP-DRS programme. RPR is thankful to U.G.C. for providing F.I.P fellowship. Authors are also thankful to the referees for critical reading of the manuscript and useful suggestions.

References

- [1] P. Nandi, G. Jose C. Jayakrishnan, S. Debbarma, K. Chalapathi, K. Alti, A. K. Dharmadhikari, J. A. Dharmadhikari, D. Mathur, *Opt. Exp* **25**, 12145 (2006).
- [2] K. Itoh, N. Kamata, T. Shimazu, C. Satoh, K. Tonooka, K. Yamada, *J. Lumin.*, **87**, 676 (2000).
- [3] N. V. Unnikrishnan, P. V. Jyothy, K. A. Amrutha, Gijo Jose, *J. fluoresc.* **19**, 165 (2009).
- [4] V. C. Costa, M. J. Lochhead, K. L. Bray **8**, 783(1996).
- [5] V. Sudarsan, Sri Sivakumar, C. J. Frank, M vanVeggel, *Chem. Mater.*, **17**, 4736(2005).
- [6] R. Reisfeld, J. Hormadaly, *J. chem. Phys.* **64**, 3207(1976).
- [7] Vinoy Thomas, Gin Jose, Gijo Jose, P.I. Paulose, N. V. Unnikrishnan *Mater. Chem. Phys* **77**, 826(2003).
- [8] C. J. Brinker, G. W. Scherer, *Sol-Gel Science: The Physics and Chemistry of sol-Gel Processing*, Academic Press(1990).
- [9] L. L. Hench, J. K. West, *Chem. Rev.* **90**, 33(1990).
- [10] A. Biswas, J. Sahu, H. N. Acharya, *Ind. J. Pure. Appl. Phys.* **34**, 993(1996).
- [11] G. N. Greaves, *J. Non. Cryst. Solids* **71**, 203 (1985).
- [12] E. Rukmini, C. K. Jayasankar, *Opt. Mat.* **4**, 529(1995).
- [13] G. Ajithkumar, P. R. Biju, N. V. Unnikrishnan, *J. Non. Cryst. Solids* **221**, 47(1997)
- [14] B. R. Judd, *Phys. Rev.* **127**, 750(1962)
- [15] G. S. Ofelt, *J. Chem Phys* **37**, 511(1962)
- [16] P. Goldner, F. Auzel *Glass J. Appl. Phys.* **10**, 7972(1996)

*Corresponding author: nvu50@yahoo.co.in